HHS Public Access

Author manuscript

Adv Mater. Author manuscript; available in PMC 2017 November 10.

Published in final edited form as:

Adv Mater. 2017 September ; 29(33): . doi:10.1002/adma.201700141.

ROS-Responsive Polyprodrug Nanoparticles for Triggered Drug Delivery and Effective Cancer Therapy

Dr. Xiaoding Xu[a], **Dr. Phei Er Saw**[a], **Dr. Wei Tao**[a], **Yujing Li**[a], **Xiaoyuan Ji**[a], **Sushant Bhasin**[a], **Dr. Yanlan Liu**[a], **Dana Ayyash**[a], **Jonathan Rasmussen**[a], **Macr Huo**[a], **Prof. Jinjun Shi**[a], and **Prof. Omid C. Farokhzad**[a],[b]

[a]Center for Nanomedicine and Department of Anesthesiology, Brigham and Women's Hospital, Harvard Medical School, Boston, MA 02115, USA

[b]King Abdulaziz University, Jeddah 21589, Saudi Arabia

Keywords

Polyprodrug; ROS-responsive; Tumor targeting; Tumor penetrating; Cancer therapy

Nanoparticle (NP)-mediated drug delivery has been widely pursued to develop safer and more effective therapeutic modalities for the treatment of a myriad of important diseases, most notably cancer.[1] Currently approved NP delivery systems such as Doxil (liposomal doxorubicin), Abraxane (NP albumin-bound paclitaxel), and Genexol-PM (paclitaxel-loaded polymer micelle) have demonstrated value in enhancing the therapeutic index of clinically validated chemotherapeutics (*e.g.*, enhancing efficacy and/or reducing toxicities),[1d, 2] but their use has not always exhibited an overall survival benefit in cancer treatment. This persistent problem is in part attributable to the suboptimal properties of NP platforms, including premature drug release during NP preparation and storage or NP circulation in blood, lack of specific tumor tissue/cell targeting, and poor tumor tissue penetration.

Over the past decade, polymer-drug conjugates, also called polymeric prodrugs, have become a fast-growing and effective approach to improve therapeutic efficacy.[3] When therapeutic drugs are conjugated to the functional groups of polymers, the resulting polymeric prodrugs show prolonged blood circulation, high stability, good water solubility, and low immunogenicity.[4] Nevertheless, because a polymer usually has a large number of functional groups, conjugation sites cannot be precisely controlled, producing product heterogeneity and variations in batch-to-batch reproducibility.[5] In recent years, the polyprodrug concept has been proposed to address this issue by polymerizing therapeutic drugs with stimuli-responsive linkers,[6] thus leading to constant and high drug-loading levels. The resulting polyprodrugs are stable and inactive under normal conditions, but can release intact drugs when stimuli such as redox or UV irradiation are applied.[6a–d, 7] Up to now, only a few polyprodrugs have been reported that achieved encouraging results both *in*

Correspondence to: Jinjun Shi; Omid C. Farokhzad.

Supporting Information

Supporting Information is available online from Wiley InterScience or from the author.

vitro and *in vivo*.[6c, 6e, 7] Nevertheless, several issues are still unsolved and hinder the clinical translation of the polyprodrug technique, especially selective accumulation at tumor site, deep tumor tissue penetration and targeted internalization by tumor cells.

Herein, we developed a new polyprodrug NP platform that is responsive to reactive oxygen species (ROS) for triggered drug delivery and effective cancer therapy. As one of the unique hallmarks of cancer, hypoxia significantly alters ROS within tumor tissue, making ROS levels much higher in cancer cells (up to 100 μM) than in normal tissue (~20 nM).[8] Therefore, unlike redox-responsive strategy that reducing agents such as glutathione (GSH) show high concentration (about 2–10 mM) in the cytoplasm of both normal and cancer cells,[9] a ROS-sensitive approach is much more tumor-specific and thus holds particular promise for enhancing the exposure of cancer cells to therapeutic molecules.[10] As a proof of concept, we chose near-infrared (NIR)-emitting anticancer drug mitoxantrone (MTO), and designed a ROS-responsive MTO-based polyprodrug (Scheme 1), which can self-assemble with lipid-polyethylene glycol (lipid-PEG) to form polyprodrug NPs. In addition, to overcome the barrier of poor tumor tissue penetration of NPs,[1d] we further employed internalizing RGD (iRGD) peptide to modify these NPs, which can target αv integrins on tumor endothelium and penetrate tumor tissues and cells via C-end Rule (CendR).[11] The resulting polyprodrug NP platform shows the following unique features (Scheme 1): i) high and stable drug loading; ii) long blood circulation attributable to the hydrophilic PEG shell; iii) specific tumor targeting and deep tumor penetrability by the surface-encoded iRGD peptide; and iv) ROS-cleavable thioketal bond in the polyprodrug for a chain-breakage patterned release of intact therapeutic drug molecules for efficient cancer therapy.

The structure of the polyprodrug is shown in Scheme 1. MTO was chosen as a model drug and co-polymerized with a ROS-cleavable thioketal-containing linker[10a, 12] (Scheme S1) to prepare the polyprodrug (denoted polyMTO, Scheme S2). As a clinically approved anticancer drug, MTO has been used for the treatment of advanced prostate cancer, acute myelogenous leukemia, and breast cancer.[13] More importantly, the NIR characteristic of MTO with excitation at 610 and 660 nm and emission at 685 nm facilitates real-time tracking of *in vitro* and *in vivo* distribution of the polyMTO-based NPs.[14] The results of nuclear magnetic resonance (NMR) analysis demonstrate the successful synthesis of polyMTO (Figure S1–S5). We also employed gel permeation chromatography (GPC) to examine the ROS response of the polyMTO which shows a molecular weight (M_n) of 8900 $gmol^{-1}$ with polydispersity (PDI) of 1.56 (Figure 1A). When the polyMTO is incubated with ROS (*e.g.*, 50 mM KO_2 solution[10a]) for 6 h, its molecular weight decreases dramatically to ~400 $gmol^{-1}$, which is closed to the molecular weight of free MTO. For comparison, we also synthesized a control polyMTO without thioketal groups (Figure S6). As can be seen in Figure S7, there is no molecular weight change for the control polyMTO after incubation with KO_2 solution for 24 h, suggesting that the degradation of polyMTO is built on the ROS-triggered cleavage of the thioketal-containing linker. This ROS response was further confirmed by high-performance liquid chromatography (HPLC). Figure 1B shows that besides several fragments of the degraded polyMTO, the retention peak corresponding to free MTO appears after incubating the polyMTO in KO_2 solution for 2 h. After further incubation for another 4 h, besides small amount of tiny fragments of degraded polyMTO, nearly all the polyprodrug molecules have degraded into free MTO, indicating that the

polyMTO undergoes a ROS-responsive elimination reaction to induce a chain-breakage patterned release of intact MTO molecules (Scheme 1A and Scheme S2).[6d, 7a, 12] Notably, because the polyMTO is a typical AB-type condensation polymer, the theoretical drug loading level can be calculated as up to around 63.7 wt% via analyzing one repeat unit in the polymer chain. This drug loading level is close to the result of our experiment (~59.4 wt%), in which the polyMTO was incubated in 50 mM KO_2 solution for 24 h and the MTO concentration was examined using fluorescence spectroscopy (E_x = 610 nm, E_m = 685 nm).

Having confirmed the ROS response of the polyMTO, we then assessed whether this polyprodrug can be used to construct stimuli-responsive NPs for on-demand drug release. With the nanoprecipitation method,[15] the polyMTO can co-assemble with DSPE-PEG_{3K} (1,2-distearoyl-*sn*-glycero-3-phosphoethanolamine-*N*-[methoxy(polyethylene glycol)-3000]) to form spherical NPs (Figure 2A), with an average hydrodynamic size of around 92 nm as determined by NanoSight (Figure S8). Moreover, these NPs are very stable, and there is nearly no drug leakage with a contant drug loading level of ~40% when placing at room temperature for one week (Figure S9). The result of *in vitro* drug release at 37 ºC further demonstrates nearly negligible drug release in the absence of ROS (Figure 2B). However, there is an improved and sustained drug release upon the addition of KO_2. Around 25% of loaded drug can be released from the NPs incubated in 50 μM KO_2 solution for 48 h. Further increasing the KO_2 concentration to 100 μM elicits around 40% release within the same time scale. With the drug release from the NPs, there is an increase in the size of the polyMTO NPs (Figure S10). In addition, this drug release also induces the increase in the fluorescence intensity the polyMTO NPs (Figure S11). Due to quenching of aggregated fluorophores the hydrophobic cores of the polyMTO NPs,[11c, 16] there is very weak fluorescence. With the ROS-triggered drug release, red fluorescence corresponding to the released MTO can be observed and the fluorescence intensity increases when prolonging the incubation time (Figure S11).

For cancer therapy, selective uptake by tumor cells is one important factor affecting ultimate therapeutic efficacy. To endow the nanoplatform with tumor-targeting ability, iRGD-conjugated DSPE-PEG_{3K} was used to decorate the polyMTO NPs (denoted as iRGD-NPs). Four prostate cancer (PCa) cell lines (PC3, DU145, 22RV1, and LNCaP) with over-expressed RGD receptors[11c, 17] were chosen to evaluate the *in vitro* tumor-targeting ability of the iRGD-NPs. In parallel, ROS generation in these PCa cells was examined by using 2′, 7′-dichlorofluorescein diacetate (DCFDA), a cell-permeable dye that is rapidly oxidized to a fluorescent molecule by intracellular ROS.[10a] Results of fluorescent microscopy (Figure S12) and flow cytometry (Figure S13) show that LNCaP cells generate higher levels of ROS than other PCa cell lines. Figures 2C and 2D present fluorescent images of LNCaP cells incubated with the non-targeted vs. targeted NPs. Both of these two NPs can be internalized by the LNCaP cells and the cellular uptake is improved as the incubation time increasing (Figure S14). With specific recognition between iRGD and αv integrins,[11a, 11c, 16] LNCaP cells show a much higher uptake of iRGD-NPs (Figure 2C) than the NPs without iRGD decoration (Figure 2D). Flow cytometry analysis (Figure S15) also confirms the tumor-targeting ability of iRGD-NPs. Mean fluorescence intensity (MFI) of the cells incubated with iRGD-NPs is > 4-fold stronger than that of cells treated with non-targeted NPs. For the

other three PCa cell lines (PC3, DU145, and 22RV1), iRGD decoration also leads to the similar effect, *i.e.*, higher cellular uptake of the iRGD-NPs (Figures S16 and S17).

Since LNCaP cells generate higher level of ROS than the other three PCa cell lines, we used this cell line to establish xenograft tumors in mice to evaluate *in vivo* tumor-targeting ability of the iRGD-NPs. Pharmacokinetics was first examined by intravenous injection of the NPs. As shown in Figure 3A, free MTO is rapidly cleared from the blood and only ~ 2% of injected MTO remains in circulation at 4 h post-injection. In contrast, the protective PEG outer layer[18] greatly extends the blood circulation time of the polyMTO NPs and makes the half-life ($t_{1/2}$) around 4.72 h. Like other RGD-modified NP systems,[11c, 16] the incorporation of iRGD peptide slightly decreases blood circulation ($t_{1/2}$ = 4.02 h) compared to the NPs without iRGD decoration. *In vivo* tumor-targeting ability was evaluated by intravenously injecting the NPs into LNCaP xenograft tumor-bearing mice (5 mg/kg, n = 3). As shown in Figure 3B, with the iRGD-mediated tumor-targeting, the iRGD-NPs display a higher tumor accumulation than the non-targeted NPs. The tumors and major organs were harvested 24 h post-injection (Figure S18), and biodistribution is shown in Figure 3C. Free MTO shows high accumulation in lung, spleen, and kidneys, but low accumulation in the tumor tissue. In contrast, due to the specific recognition between iRGD and αv integrins over-expressed on tumor cells and angiogenic tumor vasculature,[11a, 11c] the tumor accumulation of iRGD-NPs is > 5-fold or 2-fold higher than that of free MTO or non-targeted NPs, respectively.

We next evaluated the tumor-penetrating ability of the iRGD-NPs. The NPs were intravenously injected into LNCaP xenograft tumor-bearing mice (5 mg/kg), and tumors were collected 4 h post-injection and sectioned for immunofluorescence staining. As can be seen in Figure 3D, most of the NPs without iRGD decoration are positioned in or around the tumor vessels, and only a small number reach the extravascular tumor parenchyma. In contrast, a higher amount of iRGD-NPs can be visualized in the tumor section that cross tumor vessels and reach the extravascular tumor parenchyma (Figure 3E), clearly suggesting the iRGD-mediated deep tumor penetration.

Finally, we evaluated the anti-tumor efficacy of the polyMTO NPs. Their *in vitro* efficacy was assessed by examining the cytotoxicity of the NPs against PCa cell lines. Due to higher cellular uptake (Figure 2D and Figure S15), the iRGD-NPs show stronger toxicity against LNCaP cells (Figure 4A, IC_{50} = 2.69 mg/L) than the NPs without iRGD decoration (IC_{50} = 4.35 mg/L). Similar results can also be noticed in other PCa cell lines (Figure S19). Notably, unlike free MTO, which can freely and rapidly diffuse into cells, the uptake of iRGD-NPs involves endocytosis and subsequent release from endo/lysosomes, which may thus induce slightly weaker toxicity than that of free MTO against LNCaP cells (IC_{50} = 1.78 mg/L). Nevertheless, compared to free MTO, iRGD-NPs show much higher tumor accumulation *in vivo* (Figures 3B and 3C). Moreover, the iRGD decoration can improve the tumor penetration ability of the polyMTO NPs (Figure 3E). All these are important for effective cancer therapy. To validate the contribution of ROS to intracellular MTO release from polyMTO NPs, we also examined the cytotoxicity of the NPs made of control polyMTO without the ROS-responsive thioketal group (Figures S6–S8). Around 80% of PCa cells (Figures 4A and S19) are still alive even when the MTO concentration reaches 20 mg/L,

highlighting the importance of the thioketal group to the anti-tumor effect of the polyMTO NPs.

In vivo therapeutic efficacy was evaluated by intravenous injection of the polyMTO NPs into LNCaP tumor-bearing nude mice (once every three days at a 5 mg/kg MTO-equivalent dose, n = 5). As shown in Figures 4B–4D, after three consecutive injections, the iRGD-NPs show better therapeutic effect in the inhibition of tumor growth than other formulations. After 18 days, there is < 2-fold increase in tumor volume (from ~77 to ~136 mm^3), which is lower than the tumor volume increase of the mice treated by free MTO (3.3-fold increase from ~82 to ~267 mm^3) or NPs without iRGD (2.5-fold increase from ~76 to ~193 mm^3). The results of histological analysis further confirm that the iRGD-NPs are the most effective in inducing cell apoptosis (Figure 4E) while reducing cell proliferation (Figure S20). In addition, the administration of the iRGD-NPs shows no obvious effect on mouse body weight (Figure S21). To further evaluate the potential *in vivo* side effects of the polyMTO NPs, healthy mice received the injection of the NPs (5 mg/kg MTO-equivalent dose, n = 3). Blood serum analysis shows that TNF-α, IFN-γ, IL-6, and IL-12 levels are in the normal range at 24 h post injection (Figure S22). After three daily injections, multiple hematological parameters including aspartate aminotransferase (AST), alanine aminotransferase (ALT), albumin, alkaline phosphatase (ALKP), blood urine nitrogen (BUN), creatinine, and total protein are in the normal range (Figure S23). Histological analysis shows that there are no noticeable histological changes in the tissues from heart, liver, spleen, lung or kidney (Figure 24). All of these results indicate the good biocompatibility of the polyMTO NP platform.

In conclusion, we have successfully developed a new ROS-responsive and deeply tumor-penetrating polyprodrug nanoplatform for targeted cancer therapy. The polyprodrug NPs can respond to intracellular ROS with a chain-breakage patterned release of intact anticancer drug, leading to significant inhibition of tumor cell growth. The *in vitro* and *in vivo* results also demonstrate that the polyprodrug NPs can be coated with iRGD ligand to efficiently target tumors and penetrate tumor parenchyma. We expect that this ROS-responsive polyprodrug NP platform could be of high interest for on-demand delivery of other therapeutic drugs and for effective treatment of various malignancies.

Supplementary Material

Refer to Web version on PubMed Central for supplementary material.

Acknowledgments

X.X. and P.E.S. contributed equally to this work. This work was supported by the NIH grants HL127464 (O.C.F.), CA200900 (J.S.), and R00CA160350 (J.S.); the David H. Koch-Prostate Cancer Foundation (PCF) Program in Cancer Nanotherapeutics (O.C.F.); the Movember-PCF Challenge Award (O.C.F. and J.S.); the PCF Young Investigator Award (J.S.); and the National Research Foundation of Korea grant K1A1A2048701 (O.C.F.) O.C.F. has financial interest in Selecta Biosciences, Tarveda Therapeutics, and Placon Therapeutics.

References

1. a) Farokhzad OC, Langer R. ACS Nano. 2009; 3:16–20. [PubMed: 19206243] b) Petros RA, DeSimone JM. Nat Rev Drug Discov. 2010; 9:615–627. [PubMed: 20616808] c) Riehemann K, Schneider SW, Luger TA, Godin B, Ferrari M, Fuchs H. Angew Chem Int Ed. 2009; 48:872–897.d)

Shi J, Kantoff PW, Wooster R, Farokhzad OC. Nat Rev Cancer. 2017; 17:20–37. [PubMed: 27834398]

2. a) Shi J, Xiao Z, Kamaly N, Farokhzad OC. Acc Chem Res. 2011; 44:1123–1134. [PubMed: 21692448] b) Yu MK, Park J, Jon S. Theranostics. 2012; 2:3–44. [PubMed: 22272217]
3. a) Maeda H. Adv Drug Deliv Rev. 2001; 46:169–185. [PubMed: 11259839] b) Duncan R. Nat Rev Cancer. 2006; 6:688–701. [PubMed: 16900224] c) Li C, Wallace S. Adv Drug Deliv Rev. 2008; 60:886–898. [PubMed: 18374448]
4. a) Andrew MacKay J, Chen M, McDaniel JR, Liu W, Simnick AJ, Chilkoti A. Nat Mater. 2009; 8:993–999. [PubMed: 19898461] b) Mahato R, Tai W, Cheng K. Adv Drug Deliv Rev. 2011; 63:659–670. [PubMed: 21333700] c) Homsi J, Simon GR, Garrett CR, Springett G, De Conti R, Chiappori AA, Munster PN, Burton MK, Stromatt S, Allievi C, Angiuli P, Eisenfeld A, Sullivan DM, Daud AI. Clin Cancer Res. 2007; 13:5855–5861. [PubMed: 17908979] d) Du JZ, Du XJ, Mao CQ, Wang J. J Am Chem Soc. 2011; 133:17560–17563. [PubMed: 21985458] e) Kolishetti N, Dhar S, Valencia PM, Lin LQ, Karnik R, Lippard SJ, Langer R, Farokhzad OC. Proc Natl Acad Sci USA. 2010; 107:17939–17944. [PubMed: 20921363]
5. a) Christie RJ, Grainger DW. Adv Drug Deliv Rev. 2003; 55:421–437. [PubMed: 12628325] b) Duncan R, Vicent MJ. Adv Drug Deliv Rev. 2010; 62:272–282. [PubMed: 20005271] c) Miller K, Erez R, Segal E, Shabat D, Satchi-Fainaro R. Angew Chem Int Ed. 2009; 48:2949–2954.
6. a) Tang H, Murphy CJ, Zhang B, Shen Y, Van Kirk EA, Murdoch WJ, Radosz M. Biomaterials. 2010; 31:7139–7149. [PubMed: 20591475] b) Yang J, Liu W, Sui M, Tang J, Shen Y. Biomaterials. 2011; 32:9136–9143. [PubMed: 21889206] c) Zhang Y, Yin Q, Yin L, Ma L, Tang L, Cheng J. Angew Chem Int Ed. 2013; 52:6435–6439.d) Xu XD, Cheng YJ, Wu J, Cheng H, Cheng SX, Zhuo RX, Zhang XZ. Biomaterials. 2016; 76:238–249. [PubMed: 26546916] e) Li J, Ke W, Wang L, Huang M, Yin W, Zhang P, Chen Q, Ge Z. J Control Release. 2016; 225:64–74. [PubMed: 26806789]
7. a) Hu X, Hu J, Tian J, Ge Z, Zhang G, Luo K, Liu S. J Am Chem Soc. 2013; 135:17617–17629. [PubMed: 24160840] b) Hu X, Liu G, Li Y, Wang X, Liu S. J Am Chem Soc. 2015; 137:362–368. [PubMed: 25495130] c) Sun W, Li S, Häupler B, Liu J, Jin S, Steffen W, Schubert US, Butt H-J, Liang X-J, Wu S. Adv Mater. 2017; doi: 10.1002/adma.201603702
8. a) Trachootham D, Alexandre J, Huang P. Nat Rev Drug Discov. 2009; 8:579–591. [PubMed: 19478820] b) Dickinson BC, Chang CJ. Nat Chem Biol. 2011; 7:504–511. [PubMed: 21769097] c) Zhai S, Hu X, Hu Y, Wu B, Xing D. Biomaterials. 2017; 121:41–54. [PubMed: 28068593] d) Murphy, Michael P. Biochem J. 2009; 417:1–13. [PubMed: 19061483]
9. a) Schafer FQ, Buettner GR. Free Radic Biol Med. 2001; 30:1191–1212. [PubMed: 11368918] b) Cheng R, Feng F, Meng F, Deng C, Feijen J, Zhong Z. J Control Release. 2011; 152:2–12. [PubMed: 21295087]
10. a) Shim MS, Xia Y. Angew Chem Int Ed. 2013; 52:6926–6929.b) Wang M, Sun S, Neufeld CI, Perez-Ramirez B, Xu Q. Angew Chem Int Ed. 2014; 53:13444–13448.c) Yuan Y, Liu J, Liu B. Angew Chem Int Ed. 2014; 53:7163–7168.d Zhou Z, Song J, Nie L, Chen X. Chem Soc Rev. 2016; 45:6597–6626. [PubMed: 27722328] e) Qian C, Yu J, Chen Y, Hu Q, Xiao X, Sun W, Wang C, Feng P, Shen QD, Gu Z. Adv Mater. 2016; 28:3313–3320. [PubMed: 26948067] f) Saravanakumar G, Kim J, Kim WJ. Adv Sci. 2017; 4:1600124.g) Liang J, Liu B. Bioeng Transl Med. 2016; 1:239–251.
11. a) Sugahara KN, Teesalu T, Karmali PP, Kotamraju VR, Agemy L, Girard OM, Hanahan D, Mattrey RF, Ruoslahti E. Cancer Cell. 2009; 16:510–520. [PubMed: 19962669] b) Sugahara KN, Teesalu T, Karmali PP, Kotamraju VR, Agemy L, Greenwald DR, Ruoslahti E. Science. 2010; 328:1031–1035. [PubMed: 20378772] c) Xu X, Wu J, Liu Y, Yu M, Zhao L, Zhu X, Bhasin S, Li Q, Ha E, Shi J, Farokhzad OC. Angew Chem Int Ed. 2016; 55:7091–7094.
12. Wilson DS, Dalmasso G, Wang L, Sitaraman SV, Merlin D, Murthy N. Nat Mater. 2010; 9:923–928. [PubMed: 20935658]
13. D'Amico AV. J Clin Oncol. 2014; 32:362–364. [PubMed: 24344221]
14. a) Bell DH. Biochim Biophys Acta. 1988; 949:132–137. [PubMed: 3334848] b) Liu P, Qin L, Wang Q, Sun Y, Zhu M, Shen M, Duan Y. Biomaterials. 2012; 33:6739–6747. [PubMed: 22763223]

15. a) Zhang L, Chan JM, Gu FX, Rhee JW, Wang AZ, Radovic-Moreno AF, Alexis F, Langer R, Farokhzad OC. ACS Nano. 2008; 2:1696–1702. [PubMed: 19206374] b) Dehaini D, Fang RH, Luk BT, Pang Z, Hu CMJ, Kroll AV, Yu CL, Gao W, Zhang L. Nanoscale. 2016; 8:14411–14419. [PubMed: 27411852] c) Zhu X, Xu Y, Solis LM, Tao W, Wang L, Behrens C, Xu X, Zhao L, Liu D, Wu J, Zhang N, Wistuba II, Farokhzad OC, Zetter BR, Shi J. Proc Natl Acad Sci USA. 2015; 112:7779–7784. [PubMed: 26056316]
16. Wang Y, Zhou K, Huang G, Hensley C, Huang X, Ma X, Zhao T, Sumer BD, DeBerardinis RJ, Gao J. Nat Mater. 2014; 13:204–212. [PubMed: 24317187]
17. Sutherland M, Gordon A, Shnyder SD, Patterson LH, Sheldrake HM. Cancers. 2012; 4:1106–1145. [PubMed: 24213501]
18. Knop K, Hoogenboom R, Fischer D, Schubert US. Angew Chem Int Ed. 2010; 49:6288–6308.

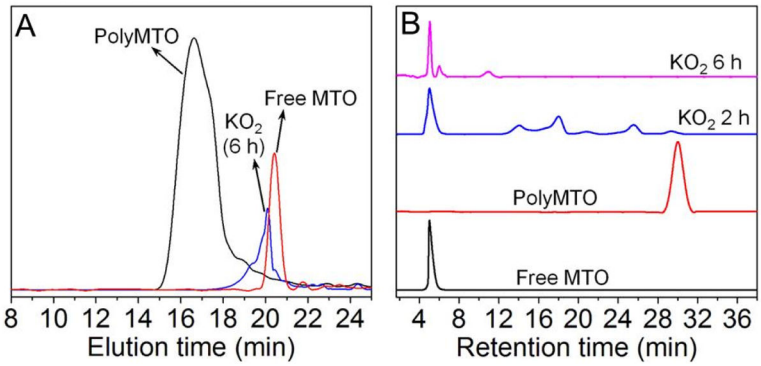

Figure 1.

(A) GPC and (B) HPLC profiles of polyMTO incubated in the mixture of DMF and H_2O (9:1, v/v) containing 50 mM KO_2.

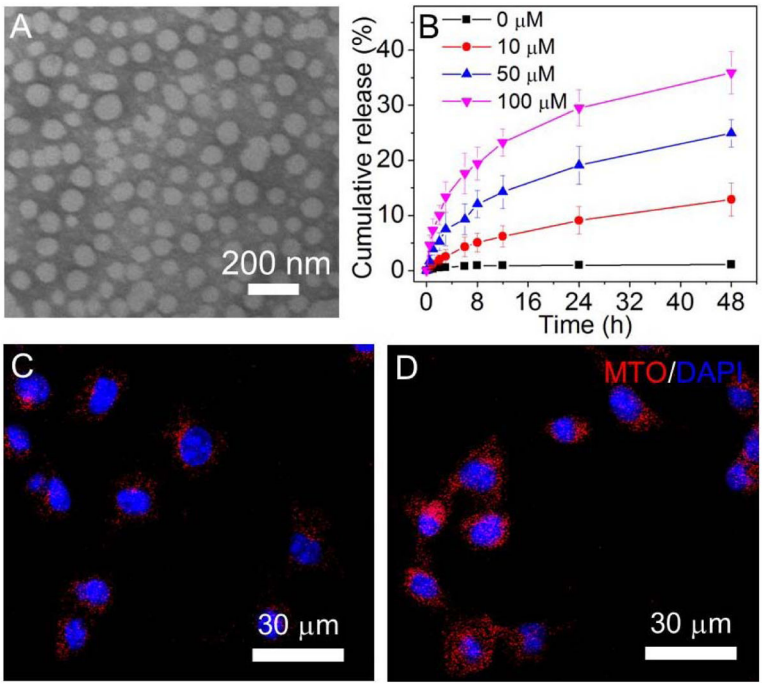

Figure 2.

(A) TEM image of the polyMTO NPs. (B) Cumulative MTO release from the polyMTO NPs incubated in PBS containing KO_2 at different concentrations. (C, D) Fluorescence images of LNCaP cells incubated with the non-targeted polyMTO NPs (C) and iRGD-NPs (D) for 4 h.

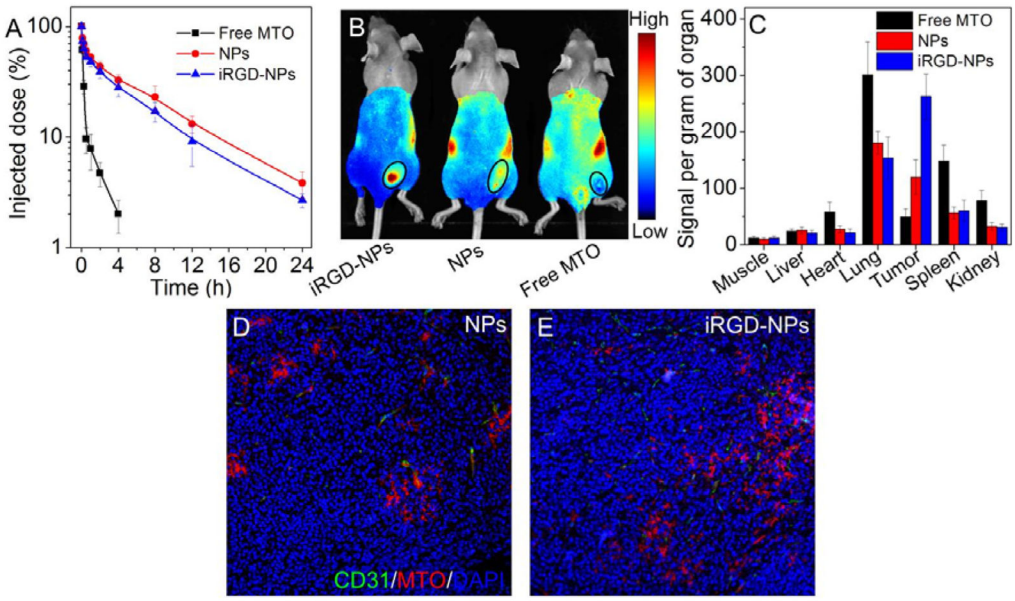

Figure 3.

(A) Pharmacokinetics of free MTO, polyMTO-based NPs and iRGD-NPs. (B) Overlaid fluorescent image of the LNCaP xenograft tumor-bearing nude mice 24 h post-injection of free MTO, polyMTO-based NPs and iRGD-NPs. Tumors are indicated by ellipses. (C) Biodistribution of free MTO and NPs in the tumors and major organs of LNCaP xenograft tumor-bearing nude mice sacrificed at 24 h post-injection. (D, E) Fluorescent images of LNCaP tumor sections at 4 h post-injection of polyMTO-based NPs (D) and iRGD-NPs (E).

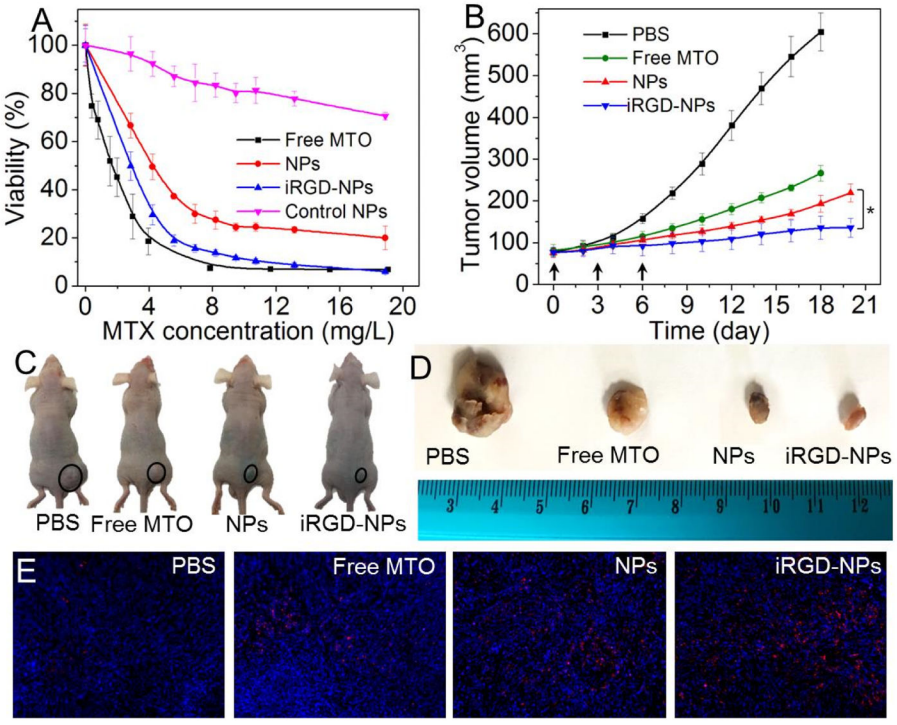

Figure 4.

(A) Cytotoxicity of free MTO, polyMTO-based NPs, iRGD-NPs, and control polyMTO NPs against LNCaP cells. (B) Tumor volume of the LNCaP xenograft tumor-bearing mice after treatment by PBS, free MTO, polyMTO-based NPs and iRGD-NPs. Intravenous injections are indicated by arrows. $*P < 0.05$. (C, D) Representative images of mice (C) and harvested LNCaP tumors (D) after treatment with PBS, free MTO, polyMTO-based NPs, and iRGD-NPs. Tumors are indicated by ellipses. (E) TUNEL staining of LNCaP tumors after treatment with PBS, free MTO, polyMTO-based NPs, and iRGD-NPs. TUNEL-positive apoptotic cells are stained with red fluorescence.

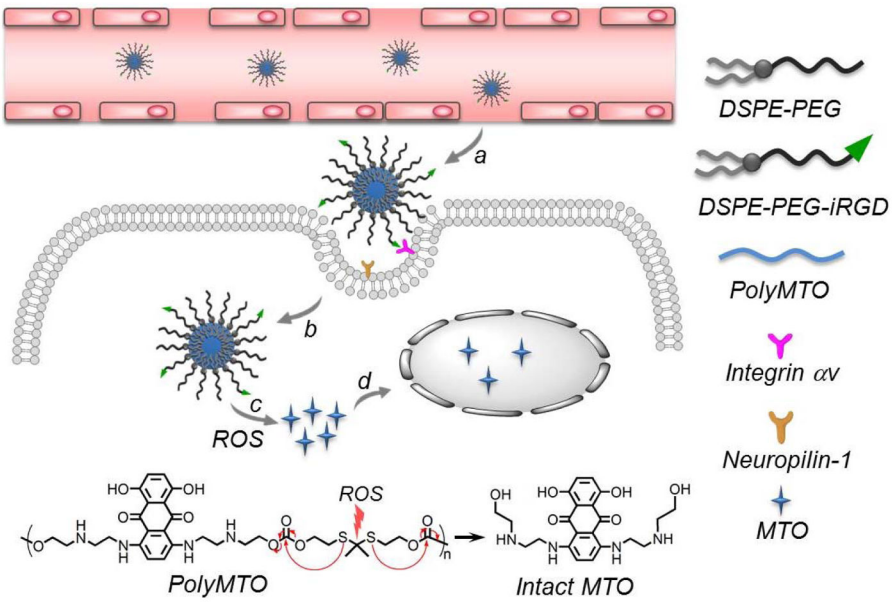

Scheme 1.

Schematic illustration of the polyMTO-based NP platform for targeted and deeply penetrating cancer therapy. After intravenous injection, the iRGD-mediated targeting strategy facilitates the tumor tissue penetration and tumor cell uptake of the NPs (*a*, *b*). Subsequently, the high level of ROS in cancer cells can break thioketal bond in the polyMTO to induce chain-breakage patterned release of intact MTO release (*c*) for disrupting DNA synthesis and efficient cancer therapy (*d*).